Table 3 Comparison of eigenvalue parameters $\bar{\mu}_i$[a]

Problem	Mode number	Number of terms (iterations) used, N	Rayleigh-Ritz method (energy principle), $\bar{\mu}_0$	Modified Rayleigh-Ritz method (complementary energy principle), $\bar{\mu}_1$	Iterated R.R. method I I-successive approximation (energy principle), $\bar{\mu}_2$	Iterated modified R.R. method (complementary energy principle,) $\bar{\mu}_3$	Iterated R.R. method II II-successive approximation (energy principle), $\bar{\mu}_4$	Stodola-Vianello iterative method
I. Torsional oscillations of uniform cantilever shaft $f_0 = \sum_{n=1}^{N} a_n x^n$	I	1	1.2159	1.013212	1.001292	1.000134	1.000015	1.2159
		2	1.007522	1.000261	1.000010	...	...	1.013212
		3	1.000137	1.000002	...	...	...	1.001292
		4	1.000001	1.000000	...	...	...	...
	II	2	1.4493	1.06075	1.01529	...	...	...
		3	1.053346	1.008759	...	...	...	...
		4	1.005185	...	...	...	...	...
	III	3	1.76933	1.12882	...	...	...	...
		4	1.125141	1.033279	...	...	...	...
		5	1.021766	...	...	...	...	...
II. Flexural oscillations of uniform cantilever beam $f_0 = \sum_{n=1}^{N} a_n x^{n+1}$	I	1	1.6178	1.00803	1.000186	...	...	1.120025
		2	1.009536	1.000016	...	...	...	1.0022612

[a] $\bar{\mu}_i = \mu_i / \mu_i$ exact.

modified Rayleigh-Ritz method. Table 3 includes results obtained by using iterative Rayleigh-Ritz type methods. This comparison shows that the accuracy increases with the increase in the number of free constants included in the trial function as well as the number of iterations. Table 4 includes a comparison of the first two successive approximation functions with the exact modes, in two typical cases. The rapid point-wise convergence is obvious in these comparisons.

Conclusions

A comparative study of Rayleigh-Ritz type and iterative type approximate methods for the evaluation of eigenvalues has been made with the aid of some simple examples. This study has brought out the relative superiority and the effectiveness of the Temple's Successive Approximation procedure. Methods based on judicious combinations of Rayleigh-Ritz and iterative methods can be highly useful in the determination of eigenvalues. The possibility of developing useful finite element analogues of the iterative Rayleigh-Ritz methods is being explored.

Table 4 Comparison of fundamental mode shapes for tapered beam

		Taper in depth only $\Lambda = 1$		Equal taper in depth and breadth $\Lambda = 1$	
x	f_0 (assumed mode shape)	First successive approximation function f_1	Exact[7]	First successive approximation function f_1	Exact[7]
0	0	0	0	0	0
0.1	0.01	0.0065	0.0062	0.0054	0.0048
0.2	0.04	0.0272	0.0259	0.0229	0.0206
0.3	0.09	0.0641	0.0613	0.0554	0.0500
0.4	0.16	0.1196	0.1148	0.1056	0.0963
0.5	0.25	0.1961	0.1891	0.1771	0.1632
0.6	0.36	0.2964	0.2874	0.2736	0.2553
0.7	0.49	0.4236	0.4133	0.3994	0.3781
0.8	0.64	0.5808	0.5709	0.5589	0.5379
0.9	0.81	0.7717	0.7648	0.7560	0.7423
1.0	1.0	1.0	1.0	1.0	1.0

References

[1] Temple, G. and Bickley, W. G., *Rayleigh's Principle*, Dover, New York, 1956.

[2] Bisplinghoff, R. L., Holt, A., and Halfman, R. L., *Aeroelasticity*, Addison-Wesley, Reading, Mass., 1955, pp. 136–138, 158–159.

[3] Collatz, L., *The Numerical Treatment of Differential Equations*, 3rd ed., Springer-Verlag, Berlin, 1960 (translated from a supplemented version of the second German edition).

[4] Martin, A. I., "Some Integrals Relating to the Vibration of a Cantilever Beam and Approximation for the Effect of Taper on Overtone Frequencies," *Aeronautical Quarterly*, Vol. VII, May 1956, pp. 109–124.

[5] Rao, J. S., "The Fundamental Flexural Vibration of a Cantilever Beam with Uniform Taper," *Aeronautical Quarterly*, Vol. XVI, May 1965, pp. 139–144.

[6] Fettis, H. E., "Torsional Vibration Modes of Tapered Bars," *Journal of Applied Mechanics*, Vol. 19, June 1952, pp. 220–222.

[7] Lindberg, G. M., "Vibration of Non-Uniform Beams," *Aeronautical Quarterly*, Vol. XIV, Nov. 1963, pp. 387–395.

[8] Mahabaliraja, "Vibrations of Tapered Beams," M.E. Project Report, 1969, Department of Aeronautical Engineering, Indian Institute of Science, Bangalore.

[9] Mabie, H. H. and Rogers, C. B., "Transverse Vibrations of Tapered Cantilever Beams with End Loads," *Journal of the Acoustical Society of America*, Vol. 36, No. 3, March 1964, pp. 463–469.

Boundary-Layer Transition and Dynamic Sting Interference

L. E. Ericsson* and J. P. Reding†

Lockheed Missiles & Space Company, Sunnyvale, Calif.

It is well known that there are difficulties associated with wind-tunnel testing at transonic speeds. However, the state-of-the-art is not as bad as is indicated by the data used

Received April 2, 1970; revision received June 17, 1970.

* Senior Staff Engineer. Associate Fellow AIAA.

† Research Specialist. Member AIAA.

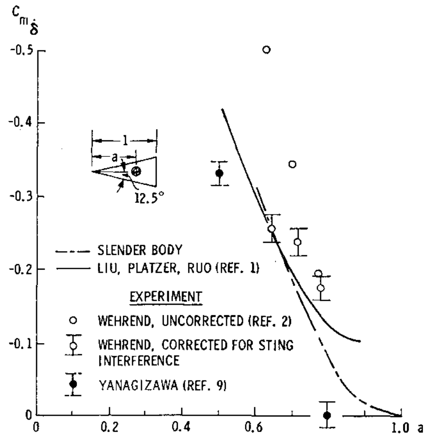

Fig. 1 Pitch damping vs pitch axis location at $M = 1$.

by Liu, Platzer, and Ruo[1] in comparing theory with experiments (Fig. 1). The experimental data spread is so large that any theory looks good. The upper set of experimental data in Fig. 1, obtained by Wehrend,[2] is shown in more detail in Fig. 2. The damping derivative should not show a nonlinear variation with angle of attack, since the static characteristics are perfectly linear. One therefore suspects that dynamic sting interference is responsible for the nonlinear distortion of Wehrend's data.

Wehrend made a thorough investigation of the effect of sting size and found that a distinct trend of increased damping with increased sting size was measured for a bulbous-based cone, whereas a flat-based model showed no effect of sting size.[2] It can be shown that a bulbous base facilitates upstream communication from the near wake to the aft body, thereby causing a dynamically destablizing effect.[3] The sharp shoulder of a flat base tends to cut off this near wake effect. The dynamic sting, largely because of its plunging, works against this undamping near wake effect.[4] The bulbous base effect is concentrated to low attitudes and amplitudes,[2,3] as is the dynamic sting interference for bulbous-based models.[4]

For a flat base, however, dynamic sting interference is observed only at hypersonic speeds when low Reynolds number flow creates a thick boundary layer that "opens up" the communication with the near wake region.[4,5] Even more powerful than a thick viscous layer is the effect of boundary-layer transition, especially when it occurs near the base (Fig. 3), when greatly increased damping results.[6,7] Boundary-layer

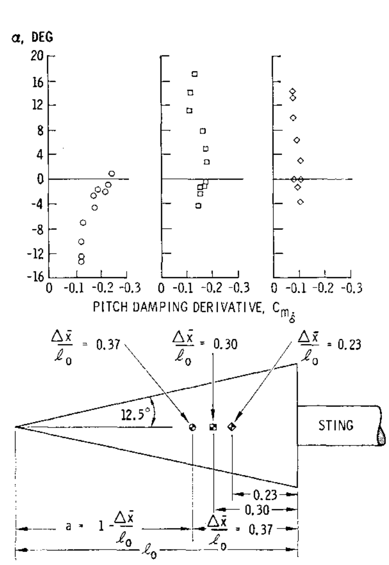

Fig. 2 Variation of pitch damping with angle of attack at $M = 1$ (Ref. 2).

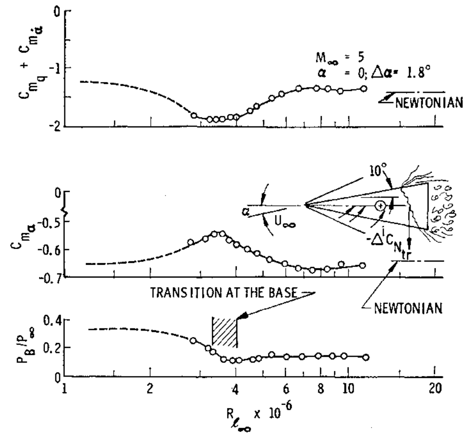

Fig. 3 Boundary-layer transition effects on sharp cone stability (Ref. 6).

transition is very sensitive to adverse pressure gradients, and it is therefore quite likely that the plunging sting could increase this damping effect of the boundary-layer transition (Fig. 4).

Checking the test Reynolds number for the sharp cone, it appears that boundary-layer transition can be expected to occur near the base for transonic Mach numbers (Fig. 5). The measured transition Reynolds number on cones in the 6×6-ft wind tunnel, the tunnel in which Wehrend's experiments were performed,[2] and in the 2×2-ft wind tunnel,

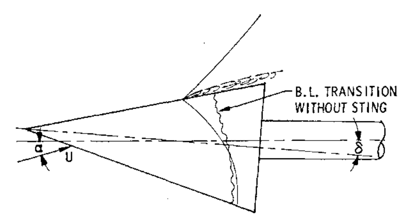

Fig. 4 Effect of plunging sting on boundary-layer transition.

which was the pilot tunnel for the 6×6-ft,[8] lies somewhat below the test Reynolds number based on body length for Wehrend's data. It is very much indicated that boundary-layer transition really occurred near the base in Wehrend's test. One would expect that a higher Reynolds number is needed for transition near the base because of the flow acceleration generated by the expansion to the near wake flow.

Thus, it is very probable that the large increase of damping at $\alpha = 0$ (Fig. 2) is caused by aft body boundary-layer transi-

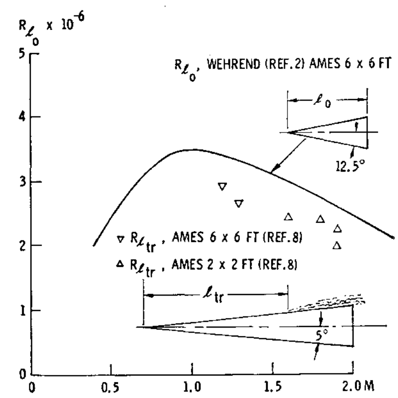

Fig. 5 Boundary-layer transition Reynolds number for cones.

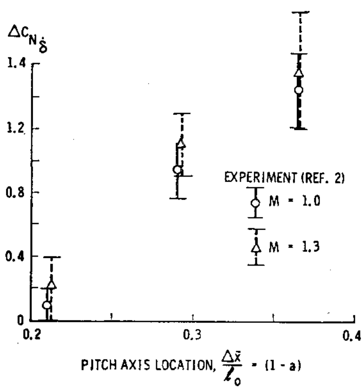

Fig. 6 Effect of pitch axis location on damping force for a 12.5° sharp cone.

tion effects. The problem is to determine how much of this increase in damping would have been observed in the absence of a sting. If one assumes that the transition-induced force is located at the base, the increased $\Delta C_{N\dot{\delta}}$ corresponding to the nonlinear increase in $C_{m\dot{\delta}}$ at $\alpha = 0$ in Fig. 2 is as shown in Fig. 6. The increase of $\Delta C_{N\dot{\delta}}$ with increasing $\Delta\bar{x}$ and consequently increased sting plunging, must be caused by sting interference. Correcting Wehrend's data for this sting interference gives vastly improved agreement with the various theories (Fig. 1). The other set of experimental data[9] is not affected by transition or support interference. Yanagizawa's results[9] were obtained using a magnetically suspended half model. It is, of course, possible that the wall boundary layer caused some interference, but another explanation for the difference between the two sets of "support-interference-free" data is the fact that Wehrend's data should be high due to the damping effect of boundary-layer transition per se,[7] in the absence of a sting.‡

References

[1] Liu, D. D., Platzer, M. F., and Ruo, S. Y., "On the Calculation of Static and Dynamic Stability Derivatives for Bodies of Revolution at Subsonic and Transonic Speeds," AIAA Paper 70-190, New York, 1970.

[2] Wehrend, W. R., Jr., "An Experimental Evaluation of Aerodynamic Damping Moments on Cones With Different Centers of Rotation," TND-1768, March 1963, NASA.

[3] Ericsson, L. E. and Reding, J. P., "Effects of Bulbous Bases on Re-Entry Vehicle Dynamics," *Transactions of the 3rd Technical Workshop on Dynamic Stability Problems*, Vol. II, Paper 6, 1968, NASA.

[4] Reding, J. P. and Ericsson, L. E., "Dynamic Support Interference on Bulbous Based Configuration," *Transactions of the 3rd Technical Workshop on Dynamic Stability Problems*, Vol. II, Paper 7, 1968, NASA.

[5] Ericsson, L. E. and Reding, J. P., "Aerodynamic Effects of Bulbous Bases," CR-1339, Aug. 1969, NASA.

[6] Ward, L. K., "Influence of Boundary-Layer Transition on Dynamic Stability at Hypersonic Speeds," *Transactions of the Second Technical Workshop on Dynamic Stability Testing*, Vol. II, Paper 9, 1965, Arnold Engineering Development Center.

[7] Ericsson, L. E., "Effect of Boundary Layer Transition on Vehicle Dynamics," *Journal of Spacecraft and Rockets*, Vol. 6, No. 12, Dec. 1969, pp. 1404–1409.

[8] Ross, A. O., "Determination of Boundary Layer Transition Reynolds Numbers by Surface-Temperature Measurement of a 10° Cone in Various NACA Supersonic Wind Tunnels," TN-3020, Oct. 1953, NACA.

[9] Yanagizawa, M., "Measurement of Dynamic Stability Derivatives of Cones and Delta-Wings at High Speeds," TR-172, 1969, National Aerospace Lab., Tokyo, Japan.

‡ In view of the present note, the results in Ref. 7 will have to be re-examined for the possibility of dynamic support interference.

First-Excursion Failure of Randomly Excited Structures: II

Y. K. Lin*
University of Illinois, Urbana, Ill.

In a recent paper[1] the probability for a randomly excited structure to survive a given service time interval $(0,t]$ without suffering a first-excursion failure was considered under rather general conditions. It was shown that the probability of survival involved the statistics of the excursion rate $N(t)$ and that an approximation to this probability derived from a necessary condition for "nonapproaching" excursions and requiring only the knowledge of the ensemble mean $E[N(t)]$ and the correlation function $E[N(t_1)N(t_2)]$ was better than the Poisson estimate (assuming independent excursions) when compared with available simulation results.[2]

The present Note is devoted to another scheme of approximation for the survival probability based on a maximum entropy principle proposed by Jaynes.[3,4] It is known that entropy is a measure of uncertainty in a random variable; therefore, an estimate of a probability distribution corresponding to the maximum entropy is the least biased estimate. This new scheme of approximation appears also to produce still better results than the nonapproaching excursion estimates.

Least Biased Estimates of Probability

It can be shown[3,4] that if our knowledge about a discrete random variable Z is limited to a number of statistics

$$E[\phi_j(Z)] = \psi_j, \quad j = 1,2,\ldots,M \tag{1}$$

then the probability $P_k = \text{Prob}\,[Z = z_k]$ corresponding to the maximum entropy is given by

$$P_k = \exp\left[-\lambda_0 - \sum_{j=1}^{M} \lambda_j\phi_j(z_k)\right] \tag{2}$$

where the constants λ are related as follows:

$$\lambda_0 = \ln\sum_k \exp\left[-\sum_j \lambda_j\phi_j(z_k)\right] \tag{3}$$

$$\frac{\partial\lambda_0}{\partial\lambda_j} = -\psi_j, \quad j = 1,2,\ldots,M \tag{4}$$

Let $\eta(t)$ be the total number of times that a structural response $X(\tau)$, $0 < \tau \leq t$, passes outside the safety region $-a \leq x \leq b$, and let the entropy of $\eta(t)$ be maximized. Since $\eta(t) = \int_0^t N(\tau)d\tau$ an application of ensemble average gives

$$E[\eta(t)] = \int_0^t g_1(\tau)d\tau \tag{5}$$

where $g_1(\tau) = E[N(\tau)]$. From Eq. (3),

$$\lambda_0 = \ln\sum_{k=0}^{\infty} \exp(-\lambda_1 k) = -\ln(1 - e^{-\lambda_1}) \tag{6}$$

Differentiate the above with respect to λ_1

$$\frac{d\lambda_0}{d\lambda_1} = e^{-\lambda_1}(e^{-\lambda_1} - 1)^{-1} = -\int_0^t g_1(\tau)d\tau, \tag{7}$$

where, in the last step, use has been made of Eq. (4) with $\int_0^t$

Received December 15, 1969; revision received July 6, 1970. The writer wishes to thank Professor Frank Kozin of the Polytechnic Institute of Brooklyn for helpful discussions and to thank his student Rimas Vaicaitis for the assistance in carrying out computations.

* Professor of Aeronautical and Astronautical Engineering. Member AIAA.